RESEARCH ARTICLE

Breaking down and building up alpha-synuclein: An insight on its N-terminal domain

Kaliroi Peqini[1] | Simone Attanasio[2] | Lucia Feni[1] | Graziella Cappelletti[2] |
Sara Pellegrino[1] ⓘ

[1]DISFARM, Dipartimento di Scienze Farmaceutiche, Sezione Chimica Generale e Organica "A. Marchesini", Università degli Studi di Milano, Milan, Italy

[2]Department of Biosciences, Università degli Studi di Milano, Milan, Italy

Correspondence
Sara Pellegrino, DISFARM, Dipartimento di Scienze Farmaceutiche, Sezione Chimica Generale e Organica "A. Marchesini", Università degli Studi di Milano, Milan 20133, Italy.
Email: sara.pellegrino@unimi.it

Funding information
European Union's Horizon 2020, Grant/Award Number: 860070

Alpha-synuclein (αSyn) is a small presynaptic protein (14 kDa) that is involved in synucleinopathies including Parkinson's disease (PD). In its native state, the αSyn monomer exists in an unfolded state, and its folding is highly dependent on variations of environmental conditions, mutations and interactions with endogenous and/or exogenous molecules. Recently, there is increasing evidence for a direct interplay between αSyn and microtubules (MTs), whose defects are linked to neurodegenerative diseases, such as PD. Understanding the correlation between αSyn and MTs could be fundamental for the correct comprehension of the undergoing mechanisms of PD. Hence, we chemically synthesized a library of peptides, deriving from both native and PD mutated sequences of the N-terminal domain of αSyn. Their secondary structure was characterized by circular dichroism and Fourier transform infrared (FTIR) experiments, in order to evaluate the effect of PD mutations. Finally, the kinetics of polymerizing tubulin in vitro in the presence of the peptides was evaluated.

KEYWORDS
conformational study, polymerization, synuclein, tubulin

1 | INTRODUCTION

Human alpha-synuclein (αSyn) is mostly expressed in the brain, especially in the neocortex, hippocampus, substantia nigra (SN), thalamus and cerebellum, and is deeply involved in PD. As demonstrated in 1997 by two seminal studies, αSyn is the main component of Lewy bodies (LB), the well-known histopathological hallmark of this neurodegenerative disorder, and secondly, its gene, *SNCA*, is mutated in familial PD.[1,2]

From a structural point of view, αSyn is a relatively small protein composed by 140 residues, and its primary sequence can be divided into three regions that are characterized by different physico-chemical properties due to their distinct amino acidic composition (Figure 1).[3,4] The N-terminal segment (residues 1–60) shows numerous amphipathic 11-mer repetitions and contains the two consensus sequences KTKEGV (spanning at residues 32–37 and 43–45). This is the αSyn region where most of the familial PD mutations are located. The non-amyloid-β-component (NAC) central region (residues 61–95) is highly amyloidogenic, giving the protein the ability to generate β-sheets. Finally, the C-terminal segment (residues 96–140) is rich in anionic residues and prevents αSyn aggregation by electrostatic repulsion.

In its native state, monomeric αSyn is unfolded, thus is commonly considered as an intrinsically disordered protein (IDP). Yet, there is still a large controversy regarding αSyn secondary and tertiary structural tendencies and the data from literature are often conflicting. Changes in the environment conditions, mutations, interactions with endogenous and/or exogenous molecules can indeed induce αSyn to fold into different structures.[5]
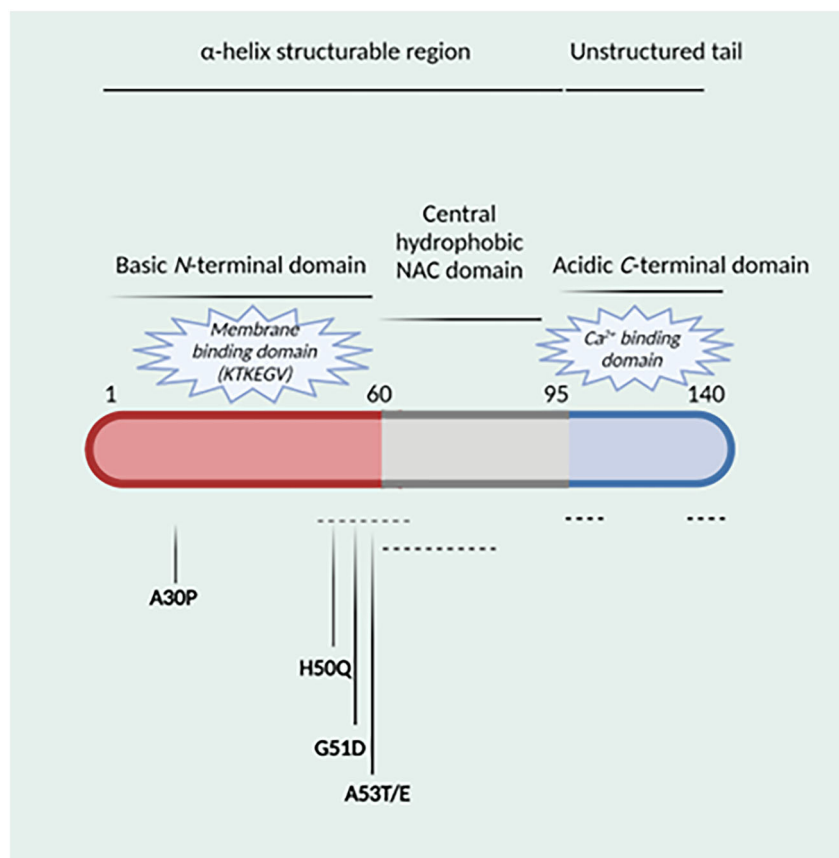
FIGURE 1 αSyn domains with highlighted PD mutations. Dash lines represent the putative domains involved in tubulin interaction.

Nowadays, there is increasing evidence for a direct interplay between αSyn and one of the principal components of cytoskeleton, that is, the microtubules (MTs), which are rigid hollow rods approximately 25 nm in diameter, consisting of repeating α-tubulin and β-tubulin heterodimers.[6] MTs are dynamic structures, and their organization and dynamics are important for the development of processes and the maintenance of the structural and functional plasticity of neurons.[7,8] Even though various research groups have studied whether αSyn directly interacts with tubulin, the binding region has not been identified so far.[9–13] Unfortunately, crystallographic structures of αSyn in complex with tubulin are not available and to date the region responsible for this interaction has not been clearly identified. As long as MTs are considered, it is known that their dynamics show strong local variations and are regulated by a large number of associated proteins that modulate their assembly state, organization and stability in a spatially restricted manner.[14] Such associated proteins include MT-associated proteins (MAPs), which bind to MT polymer on one side, and proteins such as stathmin, which bind to soluble tubulin dimers on the other, thereby shifting the polymerization/depolymerization equilibrium either to the polymer or to the dimer state.[15] It has been proposed that αSyn could interact with MTs being as well a MAP, although the results are still controversial. In one study, Alim et al. have revealed that wild-type (WT) αSyn promotes MT assembly, whereas Chen et al. have claimed that neither monomeric nor oligomeric Syn influences MT polymerization in vitro.[11,16]

Here, to get a further insight and useful tools to investigate the molecular aspects of the interaction between αSyn and tubulin, we chemically synthesized a library of peptides derived from the PD mutations prone N-terminal αSyn domain, and we evaluated their secondary structure by circular dichroism (CD) and Fourier transform infrared (FTIR) experiments in various conditions. Finally, their effect on tubulin polymerization was investigated by spectrophotometric polymerization assays.

2 | MATERIAL AND METHODS

2.1 | Materials

Usual solvents were purchased from commercial sources. Pure compounds were obtained after HPLC purification performed on a C18-Classic column, 10 μm, 250 × 21.2 mm ID (Adamas, Sepachrom). Compound purity was verified by analytical HPLC (Jasco) on a Gemini-NX, 5 μm, C18, 110A, 150 × 4.6 mm (Phenomenex). Mass spectra were acquired on Fisons MD800 spectrometer and electrospray ion trap on a Finnigan LCQ advantage thermo-spectrometer.

2.2 | Solid-phase peptide synthesis (SPPS) of αSyn protein domains

Microwave-assisted automated peptide synthesis was performed using the Fmoc/tBu protection group strategy on a Rink amide resin with a loading capacity of 0.7 mmol/g with a Liberty Blue synthesizer

using a scale of 0.1 mmol. The amino acids concentration was equal to 0.2 M in DMF.

DIC and Oxyma were used as coupling reagents (respectively 0.5 and 1 M in DMF) while for the deprotection 20% piperidine in DMF was used. For Lys, Thr, Glu, Gly, Val, Ala, Gln and Asp couplings were performed at 75°C using 170 W for 15 s and then at 90°C using 40 W for 110 s. While for His, because it is susceptible to epimerization at elevated temperatures, couplings are performed at 25°C at 0 W for 120 s and then at 50°C using 50 W for 480 s. Deprotection was performed at 75°C using 155 W for 15 s and then at 90°C using 50 W for 50 s.

2.2.1 | Cleavage from the resin

The cleavage was then performed using 3 mL of cleavage cocktail for each peptide (trifluoroacetic acid/triisopropylsilane [TIPS]/H_2O; 95:2.5:2.5) for 3 h at room temperature. After the cleavage, the peptides were precipitated from ice-cold diethyl ether and recovered by centrifugation at 4°C. Three diethyl ether washes/centrifugation cycles were carried out to efficiently remove the scavengers.

2.2.2 | Peptide purification and characterization

Peptides were purified using an ADAMAS C-18 column from Sepachrom (10 μm, 250 × 21.2 mm) by RP-HPLC using a gradient elution of 15% to 50% solvent B (solvent A: water/trifluoroacetic acid 100:0.1; solvent B: acetonitrile/trifluoroacetic acid 100:0.1) over 40 min at a flow rate of 10 mL/min. The purified peptides were freeze-dried and stored at 0°C. Afterwards, they were analysed using analytical HPLC (10% B for 3 min; 10% to 70% B over 20 min) and ESI mass spectrometry.

2.3 | Secondary structure characterization of αSyn domains

The peptides conformation was determined by CD experiments. CD experiments were performed on a Jasco J-820 spectropolarimeter with a 0.1 cm quartz cuvette. The spectra were recorded from 190 to 250 nm with a 0.2 nm step and 2 s collection time per step, taking four averages and using a sensitivity of 100 mdeg and a scanning speed of 50 nm/min. The spectrum of the solvent was subtracted to eliminate interference from cell, solvent and optical equipment. The CD spectra were plotted as mean residue ellipticity θ (degree * cm^2 * $dmol^{-1}$) versus wavelength λ (nm). Noise reduction was obtained using a Fourier transform filter program.

The peptides were measured in a concentration of 100 μM in seven different conditions:

- 100% trifluoroethanol (TFE)
- 100% phosphate buffer (NaH_2PO_4–Na_2HPO_4) at pH = 7
- 100% MES buffer at pH = 6
- 100% phosphate buffer (NaH_2PO_4–Na_2HPO_4) at pH = 8
- 50% TFE–50% phosphate buffer (NaH_2PO_4–Na_2HPO_4) at pH = 7
- 50% TFE–50% MES buffer at pH = 6
- 50% TFE–50% phosphate buffer (NaH_2PO_4–Na_2HPO_4) at pH = 8

2.4 | Attenuated total reflectance–Fourier transform infrared (ATR-FTIR) spectroscopy of αSyn peptides

FTIR spectroscopy measurements were made on a Perkin Elmer Spotlight 400 FTIR spectrophotometer equipped with a diamond crystal attenuated total reflectance (ATR) accessory. All the samples were analysed at room temperature in the solid state. A total of 32 scans were performed for all measurements with a resolution of 4 cm^{-1} in the 4000–650 cm^{-1} spectral region. Data processing was performed using OriginPro software. The deconvolution of the spectra was done in the spectral region between 1550 and 1750 cm^{-1}, using the Fit Peaks (Pro) function.

2.5 | Tubulin polymerization assay

Tubulin was obtained from an adult bovine brain, taking advantage of its polymerization/depolymerization activity in high molar Pipes buffer. The purified tubulin was then suspended in BRB buffer (80 mM K-Pipes, pH 6.9, 2 mM EGTA, 1 mM $MgCl_2$), aliquoted and stored at −80°C. Tubulin tends to spontaneously form MTs in vitro when incubated in a solution in presence of GTP at 37°C.[17] Based on this, we performed tubulin polymerization kinetics exploiting a specific kinetic tubulin assembly buffer (composed by 0.1 M Pipes, 1 mM EGTA, 0.2 mM Tris, 3 mM $MgCl_2$, pH = 6.9, 0.1 mM GTP + 10% glycerol). The buffer used to prepare the samples was degassed to avoid bubbles formation. Importantly, in order to remove cold-stable fractions and eventual aggregates formed during their storage at −80°C, tubulin aliquots were first ultra-centrifuged for 30 min at 158,000 × g (Beckman + TLA, 100.3 rotor: 54,000 rpm). Once centrifuged, the supernatant was retrieved, the protein concentration was determined with the Nanodrop ($e = 115 \times 103$ M^{-1} cm^{-1}, MW = 100 kDa, $l = 280$ nm), and then, once the concentration of the batch was verified, kinetic samples were prepared.

To investigate peptides effects, we assembled prepared 25 μM tubulin + 100 μM αSyn peptide in degassed assembly buffer + 1% DMSO. Once assembled, samples were incubated for 10 min at room temperature in the thermomixer.[12] After a gentle mixing, samples were transferred into the multiwell plate and polymerization reaction was initiated by placing the plate at 37°C into the microplate reader. Polymerization kinetics were followed for 2 h, checking the absorbance at 340 nm and maintaining a stable temperature of 37°C during the entire run.

Kinetics parameters were calculated following Cartelli et al.: initial velocity (V_i), MT assembly (ΔA) and nucleation (P).[12] V_i was determined

as the maximum change in mass over time ($\delta A/\delta t$). The ΔA was inferred based on the absorbance variation from the steady state to the sigmoidal plateau. P was calculated as the pendency of the linear part of the plot $\log(A(t)/A\infty)$ against $\log(t)$ of the sigmoidal curve.

3 | RESULTS AND DISCUSSION

3.1 | SPPS

Starting from the native αSyn sequence (Figure 2), we selected two main N-terminal sequences to be synthesized by microwave-assisted SPPS.

In order to define them, we got inspired by the recent paper of Cartelli et al.[12] In this work, it was attempted to find a tubulin-related physiological relevance for the region including the PD mutations. Pairwise alignment of WT αSyn to stathmin, a known tubulin-interacting protein, showed about 20% identical residues and over 50% conservative substitutions.[13] It has to be noted that both αSyn and stathmin weigh about 14–15 kDa and are intrinsically disordered proteins, capable of adopting α-helix conformation upon interaction with their binding partners. Interestingly, the fragment centred around αSyn residue 53 perfectly aligned to one of the functionally relevant regions of stathmin, namely, the tubulin-binding domains. This region displays multiple invariant residues, including the sites of the αSyn pathological mutation A53T, besides several other conservative or semi-conservative substitutions.

Therefore, the following N-terminal 21-residue stretches surrounding residues 30 or 53 in the αSyn polypeptide chain were selected:

→ 1) WT1 [22]TKQGVAEAAGKTKEGVLYV[40]
→ 2) WT2 [43]KTKEGVVHGVATVAEKTKEQV[63]

Furthermore, it is well known that the mutants A30P, H50Q, G51D and A53T lead to an early onset of PD and provide very different effects on the αSyn aggregation rate. As a consequence, it is particularly important to determine the effect of these mutations on the conformational behaviour of the protein domain containing the mutation.

The two WT sequences and their PD mutations were produced by MW-assisted SPPS (Table 1), using Rink amide resin as solid support (0.7 mmol/g loading). Even with the assistance of the microwaves, we faced some difficulties with their synthesis. In particular, the coupling of all the amino acids that compose the amphipathic repeated motif of αSyn KTKEQV was quite challenging. A double coupling cycle was introduced to guarantee the adequate coupling of Val to Gln, Gln to Glu, Glu to Lys, Lys to Thr and Thr to Lys (Figure 3).

However, even after following this strategy, at least one deletion was present at all crudes synthesized, affecting the crude purity.
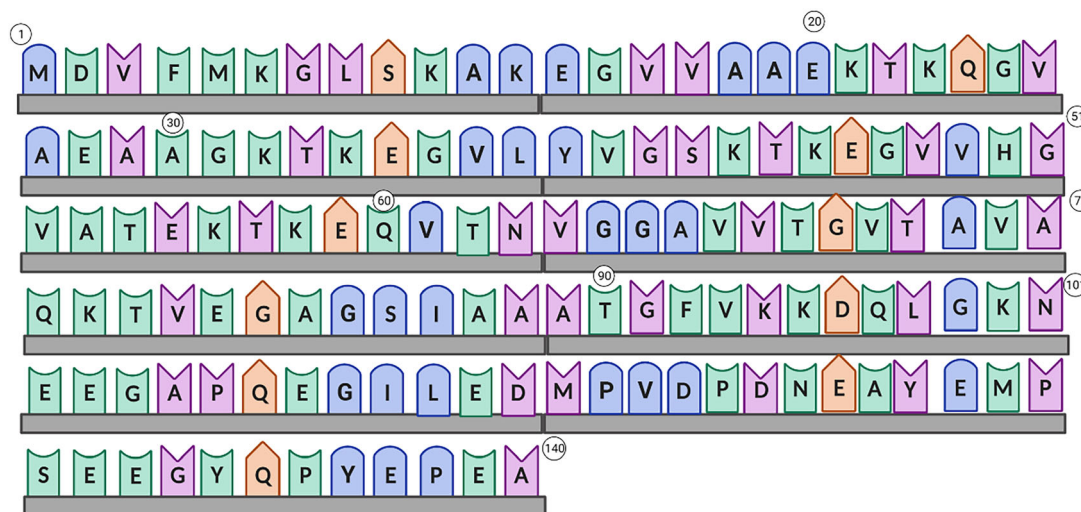

FIGURE 2 αSyn amino acid sequence.

TABLE 1 αSyn peptides synthesized with final purities, masses and yields reported.

Name	Sequence	MW cld (g/mol)	MW exp (g/mol)	Purity (%)	Mass (mg)	Yield (%)
WT1	H_2N-TKQGVAEAAGKTKEGVLYV-$CONH_2$	1947.1	1948.8	96	30.8	18
A30P	H_2N-TKQGVAEAPGKTKEGVLYV-$CONH_2$	1973.1	1972.2	96	36	21
WT2	H_2N-KTKEGVVHGVATVAEKTKEQV-$CONH_2$	2236.3	2236.4	98	21	8
A53T	H_2N-KTKEGVVHGVTTVAEKTKEQV-$CONH_2$	2266.3	2266.7	96	13.9	12
H50Q	H_2N-KTKEGVVQGVATVAEKTKEQV-$CONH_2$	2227.3	2226.7	98	7.8	3
G51D	H_2N-KTKEGVVHDVATVAEKTKEQV-$CONH_2$	2294.3	2293.8	98	10	5

FIGURE 3 Amphipathic sequence KTKEQV synthetic strategy.
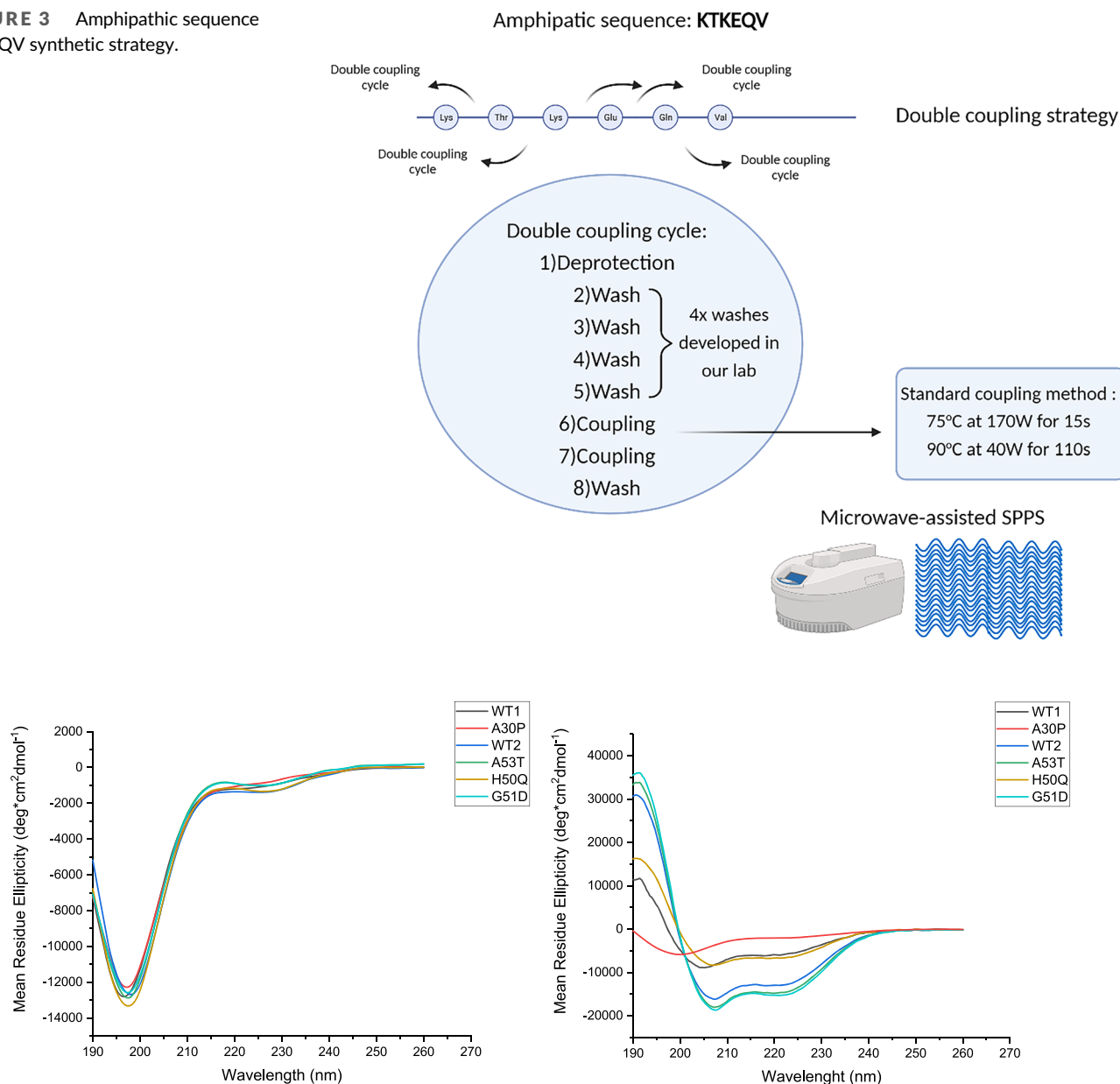
FIGURE 4 CD data from all αSyn peptides in 100% NaH$_2$PO$_4$–Na$_2$HPO$_4$ buffer at pH = 7 (left) and in 50% TFE–50% NaH$_2$PO$_4$–Na$_2$HPO$_4$ buffer at pH = 7 (right).

Most of them had indeed a purity equal to 40% to 50% (Table S1). Consequently, we run various trials of aliquots of the peptides in different eluents to verify which one is the most effective for the most efficient separation of the peaks, finding that 15% to 85% in 30 min (solvent A: water/trifluoroacetic acid 100:0.1; solvent B: acetonitrile/trifluoroacetic acid 100:0.1) allowed a good resolution of the crude.

3.2 | Structural characterization of αSyn peptides

αSyn is an intrinsically disordered protein, whose folding is highly susceptible to the environment. αSyn, indeed, tends to acquire diverse transient and dynamic conformations depending on the presence of different biological and physico-chemical factors.[5]

We performed thus the CD experiments on WT and PD mutated peptides in different conditions, to ascertain the effect of the environment and of the pH on their conformation.

For all the peptide sequences, no preferred structure could be observed in aqueous environment at different pH (Figure 4 and the Supporting Information). On the other hand, when the peptides were analysed in 50% TFE, the appearance of the typical helical signature was observed, although the effect is more evident on the WT sequences than on the mutated ones (see Supporting Information). The only exception is A53T sequence, in which the negative bands at 208 and 220 nm are more intense than the corresponding ones in

WT. On the other hand, the A30P mutation strongly affected the intrinsic helicogenity of the WT1 sequence. Analyses have been developed to deconvolute the various contributions arising from the different types of secondary structures present in a single molecule, thereby providing information on the overall structure of the peptide. The analyses were performed on the Dichroweb website using the CDSSTR algorithm for peptides in 100% NaH_2PO_4–Na_2HPO_4 buffer at pH = 7 and 100% in 50% TFE–50% NaH_2PO_4–Na_2HPO_4 buffer at pH = 7.[18] The results of these analyses can be observed in Tables 2 and 3.

Because αSyn is an IDP, we expected a combination of conformations and not just one to prevail. Indeed, in 100% NaH_2PO_4–Na_2HPO_4 buffer at pH = 7, both WT1 and WT2 conformation consisted more than 50% of random content and a mixture of other conformations. We found that quite interesting as it is in accordance with in vitro and in-cell NMR experiments which demonstrated that monomeric αSyn in solution does not possess a preferred conformation.[15] In 50% TFE, most of the peptides increased the percentage of

helical conformation, being this increase higher for WT2 and its mutated versions. This was, also, considered as a positive outcome because monomeric αSyn switches to an α-helical structure, particularly when bound to membranes or lipids or when it is in a more hydrophobic environment.[5,16–19]

Looking more in the detail to the mutations effect on the overall conformation, we could observe that in 50% TFE, the A30P mutant in comparison with WT1 undergoes a 13% loss of helical conformation and a 5% increase of random coil conformation (Table 4) (see the Supporting Information).

To further characterize the secondary structure of the peptides, we performed the ATR-FTIR analysis on the solid state (Table 5 and the Supporting Information). ATR-FTIR spectroscopy is an important method to determine secondary structure of peptides and proteins. Among the spectral regions arising out of coupled and uncoupled stretching and bending modes of amide bonds, amide I bands have been found to be the most sensitive to the variations in secondary structure folding.

TABLE 2 Percentages of secondary structure for each peptide at a concentration of 100 μM and in 100% NaH_2PO_4/Na_2HPO_4 buffer at pH = 7 calculated on Dichroweb with the CDSSTR algorithm.

Name	3-10helix (%)	α-Helix (%)	Antiparallel β-sheet (%)	Parallel β-sheet (%)	β-Turn (%)	Random (%)
WT1	1	1	17	11	16	52
A30P	1	1	17	10	15	54
WT2	0	1	17	11	12	58
A53T	1	3	20	12	18	46
H50Q	0	3	18	13	16	51
G51D	1	1	16	10	16	54

TABLE 3 Percentages of secondary structure for each peptide at a concentration of 100 μM and in 50% TFE–50% NaH_2PO_4–Na_2HPO_4 buffer at pH = 7 calculated on Dichroweb with the CDSSTR algorithm.

Name	3-10helix (%)	α-Helix (%)	Antiparallel β-sheet (%)	Parallel β-sheet (%)	β-Turn (%)	Random (%)
WT1	8	7	17	10	16	41
A30P	0	2	21	11	18	46
WT2	37	10	14	10	9	19
A53T	38	13	13	10	10	17
H50Q	10	7	14	10	19	39
G51D	38	12	13	10	11	16

TABLE 4 Percentual transition of secondary structure for mutant A30P compared with WT1 and mutants A53T, H50Q and G51D compared with WT2 at a concentration of 100 μM and in 50% TFE–50% NaH_2PO_4–Na_2HPO_4 buffer at pH = 7 calculated from data obtained on Dichroweb with the CDSSTR algorithm.

Name	3-10helix (%)	α-Helix (%)	Antiparallel β-sheet (%)	Parallel β-sheet (%)	β-Turn (%)	Random (%)
WT1 → A30P	−8	−5	+4	+1	+2	+5
WT2 → A53T	+1	+3	+1	0	+1	−2
WT2 → H50Q	−27	−3	0	0	+10	+20
WT2 → G51D	+1	+2	−1	0	+2	−3

In Table 5, we have reported the different conformations found after the deconvolution and their percentages for each peptide. By comparing these results with CD data, we can observe that in aqueous environment, the peptides are mainly unstructured, while in a hydrophobic environment, they tend to adopt a helical conformation. On the other hand, in the solid state (ATR-FTIR analysis), they adopt a mix of conformations with a prevalence of the β-sheet/aggregated strands structure.[19]

3.3 | Effects of the peptides on tubulin polymerization

To study the interplay between αSyn peptides and MTs, we investigated the impact of αSyn peptides on tubulin polymerization. We performed tubulin polymerization kinetics, an in vitro assay that allows to follow spectrophotometrically the formation of MTs from tubulin. These experiments were performed with tubulin alone (control) or in presence of tubulin together with the peptides (ratio 4:1). Importantly, before inducing MT polymerization, we pre-incubated each sample 10 min at 20°C in the thermomixer, adopting the same protocol previously published for investigating αSyn effect on tubulin polymerization.[12] After pre-incubation, kinetic tubulin assembly buffer containing GTP was added in order to induce MT polymerization, and the reaction was monitored for 2 h through a microplate reader. Then,

we analysed in detail the three parameters that allow to better understand αSyn effects on tubulin polymerization: (i) ΔA, used to indicate MT mass; (ii) V_i, describing the elongation rate of tubulin polymerization; and (iii) the P value, describing the nucleation phase.

From our experiments, we observed that only the presence of peptide WT2 or G51D affected the kinetics of the polymerization of tubulin. On the contrary, WT1, A30P and H50Q showed no major effects (see the Supporting Information). Looking more in details the WT2 curve data (V_i and ΔA values), it can be assumed that this αSyn peptide may have a pivotal role in accelerating the polymerization process, without impacting the final level of polymerized tubulin (Figure 5).

On the other side, it seems the fragment G51D impacts both the velocity of tubulin polymerization and the final level of polymerized tubulin (Table 6).

TABLE 6 Values of ΔA, V_i and P value for tubulin alone, tubulin in the presence of WT2 and in the presence of G51D.

	Tub DMSO	WT2	G51D
ΔA	0.2276	0.2116	0.0919
V_i	0.0027	0.0037	0.0007
P value	2.8369	1.86215	2.4795

TABLE 5 Percentages of secondary structure for each peptide at the solid state calculated with OriginPro.

Name	3-10helix (%)	α-Helix (%)	Antiparallel β-sheet (%)	Parallel β-sheet (%)	Aggregated strands (%)	Random (%)
WT1	41	-	3	36	17	-
A30P	-	-	30	70	-	-
WT2	-	43	12	44	-	-
A53T	-	26	11	-	61	-
H50Q	-	-	14	-	54	31
G51D	28	-	20	-	52	-

FIGURE 5 Polymerization of tubulin, in the presence of DMSO alone (Tub + DMSO), WT2 and G51D.
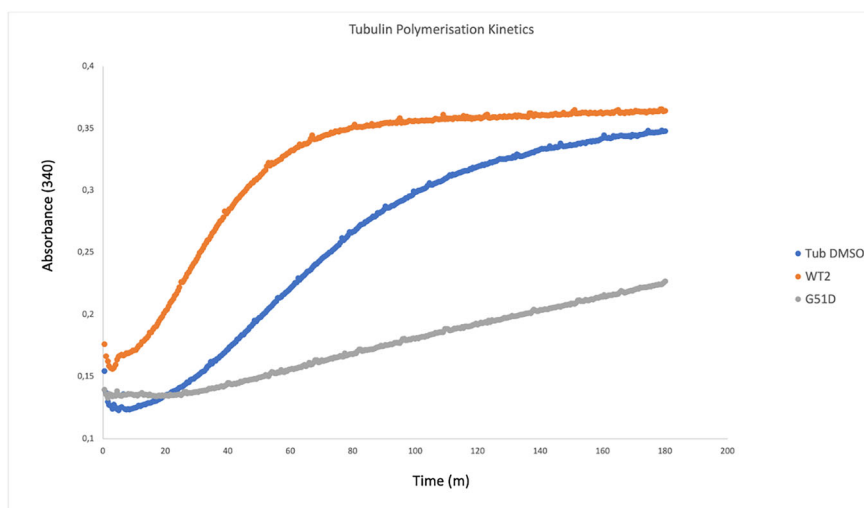
4 | CONCLUSIONS

In this work, we presented the chemical synthesis of different N-terminal protein domains related to αSyn and its PD mutated versions. The conformational evaluation allowed to determine an intrinsic helicogenic behaviour in solution, whose extent depends on the primary sequence and thus on the presence of different PD mutations. The effect of the N-terminal peptides on tubulin polymerization was also evaluated indicating a role of the 43–63 region and opening new scenarios in the evaluation of specific regions of αSyn that interact with tubulin. Further studies, however, warrant to supply further empirical tests to comprehensively elucidate the nature of this dynamic interaction.

AUTHOR CONTRIBUTIONS

Sara Pellegrino and Graziella Cappelletti conceived the research; Kaliroi Peqini synthesized the peptides; Kaliroi Peqini and Lucia Feni performed IR and CD conformational analyses; Kaliroi Peqini and Simone Attanasio performed polymerization assays; Sara Pellegrino and Kaliroi Peqini wrote the article. All authors reviewed the article.

ACKNOWLEDGEMENTS

CONFLICT OF INTEREST STATEMENT

All authors declare no conflict of interest.

ORCID

Sara Pellegrino https://orcid.org/0000-0002-2325-3583

REFERENCES

1. Polymeropoulos MH, Lavedan C, Leroy E, et al. Mutation in the α-synuclein gene identified in families with Parkinson's disease. *Science*. 1997;276(5321):2045-2047. doi:10.1126/science.276.5321.2045
2. Spillantini MG, Schmidt ML, Lee VM, Trojanowski JQ, Jakes R, Goedert M. α-Synuclein in Lewy bodies. *Nature*. 1997;388(6645):839-840. doi:10.1038/42166
3. Fusco G, De Simone A, Gopinath T, et al. Direct observation of the three regions in α-synuclein that determine its membrane-bound behaviour. *Nat Commun*. 2014;5(1):3827. doi:10.1038/ncomms4827
4. Uversky VN, Eliezer D. Biophysics of Parkinson's disease: structure and aggregation of α-synuclein. *Curr Protein Pept Sci*. 2009;10(5):483-499.
5. Bisi N, Feni L, Peqini K, et al. α-Synuclein: an all-inclusive trip around its structure, influencing factors and applied techniques. *Front Chem*. 2021;9:666585. doi:10.3389/fchem.2021.666585
6. Mazzetti S, Calogero AM, Pezzoli G, Cappelletti G. Cross-talk between α-synuclein and the microtubule cytoskeleton in neurodegeneration. *Exp Neurol*. 2023;359:114251. doi:10.1016/j.expneurol.2022.114251
7. Mitchison T, Kirschnert M. Cytoskeletal dynamics and nerve growth. *Neuron*. 1988;1(9):761-772. doi:10.1016/0896-6273(88)90124-9
8. Hahn I, Voelzmann A, Liew YT, Costa-Gomes B, Prokop A. The model of local axon homeostasis—explaining the role and regulation of microtubule bundles in axon maintenance and pathology. *Neural Dev*. 2019;14(1):11. doi:10.1186/s13064-019-0134-0
9. Payton JE, Perrin RJ, Clayton DF, George JM. Protein–protein interactions of alpha-synuclein in brain homogenates and transfected cells. *Mol Brain Res*. 2001;95(1–2):138-145. doi:10.1016/S0169-328X(01)00257-1
10. Alim MA, Hossain MS, Arima K, et al. Tubulin seeds α-synuclein fibril formation. *J Biol Chem*. 2002;277(3):2112-2117. doi:10.1074/jbc.M102981200
11. Alim MA, Ma Q-L, Takeda K, et al. *Demonstration of a Role for α-Synuclein as a Functional Microtubule-Associated Protein*. Vol. 6. IOS Press; 2004.
12. Cartelli D, Aliverti A, Barbiroli A, et al. α-Synuclein is a novel microtubule dynamase. *Sci Rep*. 2016;6(1):33289. doi:10.1038/srep33289
13. Zhou RM, Huang YX, Li XL, et al. Molecular interaction of α-synuclein with tubulin influences on the polymerization of microtubule in vitro and structure of microtubule in cells. *Mol Biol Rep*. 2010;37(7):3183-3192. doi:10.1007/s11033-009-9899-2
14. Gudimchuk NB, McIntosh JR. Regulation of microtubule dynamics, mechanics and function through the growing tip. *Nat Rev Mol Cell Biol*. 2021;22(12):777-795. doi:10.1038/s41580-021-00399-x
15. Avila J, Domínguez J, Díaz-Nido J. Regulation of microtubule dynamics by microtubule-associated protein expression and phosphorylation during neuronal development. *Int J Dev Biol*. 1994;38(1):13-25.
16. Chen L, Jin J, Davis J, et al. Oligomeric α-synuclein inhibits tubulin polymerization. *Biochem Biophys Res Commun*. 2007;356(3):548-553. doi:10.1016/j.bbrc.2007.02.163
17. Castoldi M, Popov AV. Purification of brain tubulin through two cycles of polymerization–depolymerization in a high-molarity buffer. *Protein Expr Purif*. 2003;32(1):83-88. doi:10.1016/S1046-5928(03)00218-3
18. Sreerama N, Woody RW. Estimation of protein secondary structure from circular dichroism spectra: comparison of CONTIN, SELCON, and CDSSTR methods with an expanded reference set. *Anal Biochem*. 2000;287(2):252-260. doi:10.1006/abio.2000.4880
19. Ji Y, Yang X, Ji Z, et al. DFT-calculated IR spectrum amide I, II, and III band contributions of *N*-methylacetamide fine components. *ACS Omega*. 2020;5(15):8572-8578. doi:10.1021/acsomega.9b04421

SUPPORTING INFORMATION

Additional supporting information can be found online in the Supporting Information section at the end of this article.